Direct and indirect band gap room temperature electroluminescence of Ge diodes

M. de Kersauson,[1] R. Jakomin,[2] M. El Kurdi,[2,a)] G. Beaudoin,[2] N. Zerounian,[2] F. Aniel,[2] S. Sauvage,[2] I. Sagnes,[2] and P. Boucaud[2,b)]
[1]*Institut d'Electronique Fondamentale, CNRS, Univ Paris-Sud 11, Bâtiment 220, F-91405 Orsay, France*
[2]*Laboratoire de Photonique et de Nanostructures, CNRS, Route de Nozay, 91460 Marcoussis, France*

(Received 22 March 2010; accepted 8 June 2010; published online 26 July 2010)

Germanium is a promising material for electrically pumped light emitters integrated on silicon. In this work, we have investigated the room temperature electroluminescence of pure germanium diodes grown by metal organic chemical vapor deposition. The dependence of the optical response of the *p*-*n* diodes is studied as a function of the injected current. Both direct and indirect band gap recombinations are observed at room temperature around 1.6 and 1.8 μm. The amplitude of the direct band gap recombination is equivalent to the one of the indirect band gap. © *2010 American Institute of Physics*. [doi:10.1063/1.3462400]

I. INTRODUCTION

Different approaches have been investigated for light emission on a silicon platform. Heterogeneous integration of III-V materials is obviously a promising approach. Alternatives using group IV elements are also particularly interesting in reason of their intrinsic compatibility with silicon technology. A Raman laser has been demonstrated using silicon-on-insulator waveguides and ring resonators.[1,2] One drawback of the Raman approach is that, apart from the requirement of optical pumping, long interaction lengths are required to achieve lasing. Photonic crystals represent an option to achieve compact optically-pumped lasers on silicon.[3] Silicon germanium alloys[4] and self-assembled islands[5–7] have also been considered as potential light emitters. The recombination efficiency remains however limited by the indirect band gap character of the alloys. More recently, pure germanium has gained a considerable interest since pure germanium is a "quasidirect" band gap material as compared to silicon. The energy splitting between the conduction *L* valley and zone center Gamma valley is only 140 meV at room temperature. Moreover, the recombination properties of germanium can be tailored by several methods. *N*-type doping of germanium leads to an enhanced room temperature optical recombination associated with the direct band gap due to the increase in the conduction Fermi level.[8,9] Tensile strain can reduce the energy splitting between the *L* and Gamma valleys and leads to a more efficient population of the zone center valley. A transition from indirect to direct band gap has been predicted for a biaxial tensile strain around 2%.[10] Tensile strain can be obtained by several methods, either using the difference of thermal expansion coefficients between Ge and Si (Ref. 11) or by applying a mechanical external strain.[12,13] Strong optical gain has been theoretically predicted for direct band gap tensile strained germanium.[13–16] Experimentally, optical studies of tensile strained *n*-doped germanium or Ge quantum wells have demonstrated optical gain at room temperature.[17,18] These advances have culminated in the recent demonstration of a Ge laser on silicon operating at room temperature under optical pumping, thus leading to a new paradigm for the development of optical sources on silicon.[19] The next important step is obviously to demonstrate a laser under electrical injection. As a result, germanium *p*-*n* homojunction diodes on silicon have been recently investigated.[20,21] In the latter cases, the optical response was analyzed for wavelengths shorter than 1.65 μm because of the detector cut-off used to detect the luminescence. In this way, only the recombination at high energy associated with the direct band gap can be observed. Moreover, the weight of the indirect band gap recombination on the luminescence amplitude and the precise knowledge of the recombination maximum cannot be accurately estimated.

In this work, we investigate the electroluminescence of pure germanium diodes. The *p*-*n* diodes are grown by metal organic chemical vapor deposition on a germanium substrate. The epitaxy reactor can handle both III-V and group IV elements, thus allowing the growth of germanium on GaAs or the growth of GaAs on germanium. The epitaxial growth of both *p* and *n*-doped germanium layers allows to achieve abrupt junctions and to optimize the doping content.[22] We investigate the room temperature electroluminescence as a function of the injection current. The optical response is analyzed on a broad spectral range, not only below 1.65 μm. We are thus able to observe both the direct band gap and the indirect band gap recombinations. We show that the amplitude of the recombination between direct and indirect band gaps is of the same order of magnitude. The broad spectral range that is covered allows to determine the position of the electroluminescence maximum which is correlated with the device temperature.

II. GERMANIUM DIODES

The growth of the diodes was performed on a *n*-doped germanium substrate (doping 10^{18} cm^{-3}) by metal organic

a)Electronic mail: moustafa.el-kurdi@ief.u-psud.fr.
b)Electronic mail: philippe.boucaud@ief.u-psud.fr.

 © 2010 American Institute of Physics

Downloaded 28 Jul 2010 to 193.48.163.6. Redistribution subject to AIP license or copyright; see http://jap.aip.org/jap/copyright.jsp

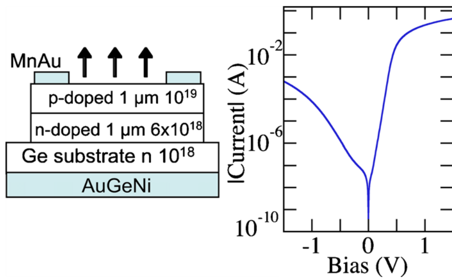

FIG. 1. (Color online) Left: schematic representation of the investigated diode (sample 152). The doping densities are per cubic centimeter. The size of the MnAu ring contact is 40 μm. Right: room temperature current-voltage characteristic of a diode. The diode diameter is 150 μm.

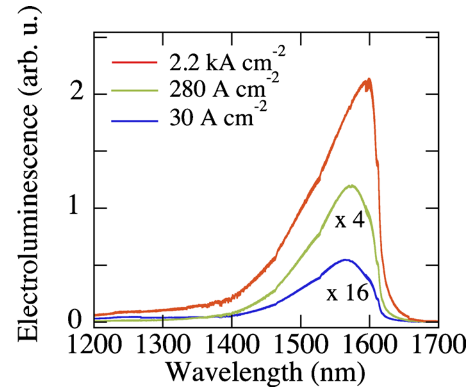

FIG. 2. (Color online) Room temperature electroluminescence of a 150 μm diameter diode for different current densities. The emission is measured with a linear InGaAs array. The cut-off at 1600 nm is due to the InGaAs array.

chemical vapor deposition using isobutyl germane (IBGe) as precursor.[23] Hydrogen is used as carrier gas with a total transport flow of 55 000 SCCM/min (SCCM denotes standard cubic centimeter per minute). The reactor pressure was set at 70 Torr and the growth temperature at 670 °C. The n-type doping was obtained with arsine gas (AsH_3) and p-type doping was achieved with trimethylgallium. Different stackings were investigated. The thickness of n-type layer was 1 μm with a doping of 6×10^{18} cm^{-3} (sample 152) or 1×10^{19} cm^{-3} (sample 153). The thickness of the p-type layer was 1 μm with a doping of 1×10^{19} cm^{-3}. The doping densities were measured by Hall effect and secondary ion mass spectroscopy. The diodes were processed into mesas with different diameters varying between 150 to 800 μm. A MnAu ring contact was deposited on top of the p-type layer. An AuGeNi contact was deposited on the backside of the substrate. The electroluminescence was measured at room temperature under continuous wave electrical injection. The emission was collected with $\times$40 objective lens with a numerical aperture of 0.6. It was detected either with a liquid-nitrogen cooled InGaAs linear array photodetector or a liquid-nitrogen cooled InSb photodetector. The InSb detector has a much lower detectivity at 1.6 μm wavelength as compared to InGaAs but exhibits a cut-off wavelength around 5 μm. It thus allows to investigate both the direct and indirect band gap recombinations between 1.5 and 2.5 μm.

III. RESULTS

Figure 1 shows a characteristic I-V curve of the 152 sample measured on a 150 μm diameter mesa. A typical diode-like behavior is observed. At a reverse bias of -1 V, the dark current is around 70 μA. The dark current increases as the diode size increases. Before the onset of tunnel injection below -0.3 V, the dark current scales with the diode surface. The onset of high level injection of the diode is 0.4 V. Below 0.4 V, the diode has an ideality factor of 1.16. In this regime, the current scales with the diode diameter. It indicates that the electric field distribution is not uniform. This feature was confirmed by the spatial mapping of electroluminescence for diodes with large diameters which exhibits an inhomogeneous electroluminescence distribution. Above 0.4 V, the resistance of the global device is 2.3 Ω. Similar results were obtained for the sample with the higher doped n-type layer.

Figure 2 shows the electroluminescence spectra of a p-n homojunction (sample 152) as measured with an InGaAs linear array. The spectra correspond to typical electroluminescence recombination spectra as reported in Refs. 20 and 21. The current density is obtained by the ratio between the current intensity and the mesa surface. At weak current density, the maximum of electroluminescence is observed around 1565 nm, corresponding to the direct band gap of germanium. As the current density increases, the maximum shifts to long wavelength as a result of thermal heating of the sample. The sharp drop around 1600 nm is due to the detector cut-off which prevents the accurate measurement of the maximum at high current densities. Moreover, the contribution from direct band gap and indirect band gap becomes difficult to disentangle at high injected current densities. For these reasons, we have measured the electroluminescence spectra with a broad band InSb photodetector. The much lower detectivity as compared to InGaAs is compensated by the large spectral range. Figure 3 shows typical spectra obtained for a current density of 0.55 and 2.2 kA cm^{-2} for sample 152 and diode diameter of 150 μm. The direct band gap recombination is clearly observed around 1600 nm.

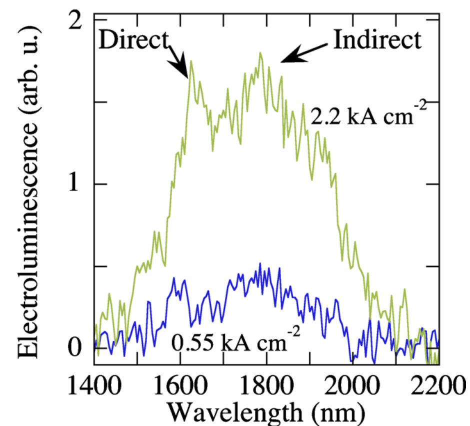

FIG. 3. (Color online) Electroluminescence spectra measured for two different current injection densities [0.55 (bottom) and 2.2 kA cm^{-2} (top)]. The emission is detected with a broad band InSb photodetector. The direct band gap recombination is observed around 1600 nm. The maximum of indirect band gap recombination is around 1800 nm. These extrema are indicated by arrows.

Downloaded 28 Jul 2010 to 193.48.163.6. Redistribution subject to AIP license or copyright; see http://jap.aip.org/jap/copyright.jsp

Meanwhile, the recombination associated with the indirect band gap has a significant contribution to the measured signal. This feature was already pointed out in Ref. 24. The indirect band gap resonance occurs around 1.8 μm. We note that the amplitude of the collected direct band gap recombination is decreased by the reabsorption which is efficient for a direct recombination. At room temperature, the indirect band gap recombination results from no phonon recombination where the momentum conservation is obtained through carrier scattering processes and phonon-assisted recombination. With the InSb photodetector we can follow the maximum of the direct band gap which shifts from 1565 to 1630 nm at 2.2 kA cm^{-2}. The striking feature is that the room temperature direct band gap recombination amplitude is not significantly different from the indirect band gap even at high current densities. It indicates that tensile strain is really mandatory to achieve population inversion with this material. Without strain enhancement, the bulk germanium has not a recombination efficiency better than the one of an indirect band gap material.

The similar amplitude between indirect and direct band gap recombinations can be compared to the expected one obtained from the theoretical emission spectrum. According to the Van Roosbreck–Schockley relation, the recombination rate at equilibrium can be calculated from the absorption spectrum and the photon density of states.[25,26] The indirect band gap absorption in doped semiconductor is enhanced as compared to the intrinsic absorption since impurity scattering and carrier-carrier scattering provide additional mechanisms to satisfy the wave vector conservation rule during an absorption or emission process. Consequently, the difference between direct and indirect absorption magnitude is less marked in doped semiconductors as compared to intrinsic semiconductors since phonon-assisted transitions are not the only mechanisms for wave vector conservation. For a *p-n* junction, the recombination is still a Planckian radiation enhanced exponentially by the applied voltage. Using the experimental absorption spectra in doped germanium reported by Pankove and Aigrain,[27] the calculation of the recombination rate in a 5×10^{18} cm^{-3} *n*-doped germanium layer indicates that the amplitude between indirect and direct band gap recombination is roughly equivalent at room temperature, as measured experimentally. The same calculation in intrinsic germanium shows that the direct band gap recombination, without accounting for reabsorption, is larger by a factor of 2 than the indirect band gap recombination.[24] The experimental spectral positions of the maxima are also in satisfying agreement with the calculated ones, if we account for temperature increase at high injection and the effects of band gap narrowing due to doping.

Figure 4(a) shows the integrated electroluminescence intensity as a function of current density. A linear dependence of the electroluminescence intensity is observed up to 2.2 kA cm^{-2}. This indicates that the recombination is dominated by the recombination of minority carriers. Similar results were obtained for the 153 sample. We did not observe any non linear dependence of the electroluminescence as reported in Refs. 20 and 21. The nonlinear behavior was attributed to a more efficient scattering of carriers in the Gamma

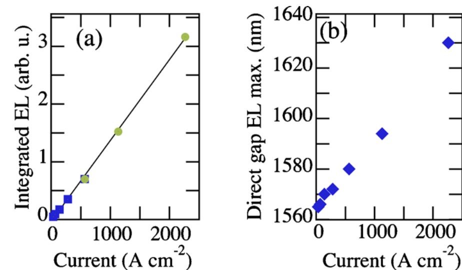

FIG. 4. (Color online) (a) Integrated electroluminescence intensity as a function of current density. The full line is a guide to the eyes. The data obtained below (above) 560 A cm^{-2} are measured with the InGaAs (InSb) detector. The two data points at 560 A cm^{-2} have been arbitrarily adjusted to the same value. (b) Direct band gap electroluminescence maximum as a function of current density.

valley as the current density increases. As compared to the latter studies where the Ge diodes were fabricated on a silicon substrate, the thermal dissipation and carrier recombination dynamics are likely to be different. Moreover, no residual tensile strain is present in the investigated diodes. Figure 4(b) shows the dependence of the direct band gap extremum as a function of the current density. The increase in current density has a direct impact on the device temperature. At 2.2 kA cm^{-2}, the device temperature is estimated from the temperature dependence of the direct band gap. The maximum of photoluminescence for a direct band gap semiconductor is expected at $E_g+k_BT/2$, corresponding to a temperature increase of 90 K for a 2.2 kA cm^{-2} injected current density as compared to a weak excitation density. This temperature increase is not necessarily a limitation for the operation of an electrically injected laser. An increased temperature reduces the splitting between the Gamma and *L* valley ($\sim$6 meV for a temperature increase of 100 K) and thus allows to obtain a higher gain for a fixed current injection density. This behavior is in contrast with the one of standard semiconductor lasers. In the case of germanium, the temperature is also a key parameter for the operation of an electrically injected device.

IV. CONCLUSION

We have reported on electroluminescence characteristics of germanium homojunction diodes grown by metal organic chemical vapor deposition. The large investigated spectral range allows to observe simultaneously direct and indirect band gap optical recombinations. The amplitude of the direct band gap recombination is of the same order of magnitude than the amplitude of the indirect band gap. The enhancement of the recombination through tensile strain is thus a very important feature to achieve lasing under electrical injection. For the development of electrically pumped lasers, the cavities could be provided by standard Fabry–Perot resonators or two-dimensional photonic crystals.[28,29]

ACKNOWLEDGMENTS

This work was partly supported by the French Ministry of Industry under Nano2012 convention, by “Triangle de la Physique” and by the seventh European PCRD project APOLLON.

Downloaded 28 Jul 2010 to 193.48.163.6. Redistribution subject to AIP license or copyright; see http://jap.aip.org/jap/copyright.jsp

[1]H. S. Rong, A. S. Liu, R. Jones, O. Cohen, D. Hak, R. Nicolaescu, A. Fang, and M. Paniccia, Nature (London) **433**, 292 (2005).
[2]H. Rong, S. Xu, Y.-H. Kuo, V. Sih, O. Cohen, O. Raday, and M. Paniccia, Nat. Photonics **1**, 232 (2007).
[3]X. Checoury, M. El Kurdi, Z. Han, and P. Boucaud, Opt. Express **17**, 3500 (2009).
[4]J. C. Sturm, H. Manoharan, L. C. Lenchyshyn, M. L. W. Thewalt, N. L. Rowell, J.-P. Noël, and D. C. Houghton, Phys. Rev. Lett. **66**, 1362 (1991).
[5]C. Hernandez, Y. Campidelli, D. Simon, D. Bensahel, I. Sagnes, G. Patriarche, P. Boucaud, and S. Sauvage, J. Appl. Phys. **86**, 1145 (1999).
[6]V. Yam, V. Le Thanh, Y. Zheng, P. Boucaud, and D. Bouchier, Phys. Rev. B **63**, 033313 (2001).
[7]T. Brunhes, P. Boucaud, S. Sauvage, F. Aniel, J. M. Lourtioz, C. Hernandez, Y. Campidelli, O. Kermarrec, D. Bensahel, G. Faini, and I. Sagnes, Appl. Phys. Lett. **77**, 1822 (2000).
[8]X. Sun, J. Liu, L. C. Kimerling, and J. Michel, Appl. Phys. Lett. **95**, 011911 (2009).
[9]M. El Kurdi, T. Kociniewski, T.-P. Ngo, J. Boulmer, D. Debarre, P. Boucaud, J. F. Damlencourt, O. Kermarrec, and D. Bensahel, Appl. Phys. Lett. **94**, 191107 (2009).
[10]R. Soref, J. Kouvetakis, and J. Menendez, Mat. Res. Soc. Symp. Proc. **958**, 13 (2007).
[11]Y. Ishikawa, K. Wada, D. D. Cannon, J. Liu, H.-C. Luan, and L. C. Kimerling, Appl. Phys. Lett. **82**, 2044 (2003).
[12]M. El Kurdi, H. Bertin, E. Martincic, M. de Kersauson, G. Fishman, S. Sauvage, A. Bosseboeuf, and P. Boucaud, Appl. Phys. Lett. **96**, 041909 (2010).
[13]P. H. Lim, S. Park, Y. Ishikawa, and K. Wada, Opt. Express **17**, 16358 (2009).
[14]J. Liu, X. Sun, D. Pan, X. Wang, L. C. Kimerling, T. L. Koch, and J. Michel, Opt. Express **15**, 11272 (2007).
[15]G. Pizzi, M. Virgilio, and G. Grosso, Nanotechnology **21**, 055202 (2010).
[16]M. El Kurdi, G. Fishman, S. Sauvage, and P. Boucaud, J. Appl. Phys. **107**, 013710 (2010).
[17]J. Liu, X. Sun, L. C. Kimerling, and J. Michel, Opt. Lett. **34**, 1738 (2009).
[18]C. Lange, N. S. Koster, S. Chatterjee, H. Sigg, D. Chrastina, G. Isella, H. von Kanel, M. Schafer, M. Kira, and S. W. Koch, Phys. Rev. B **79**, 201306 (2009).
[19]J. Liu, X. Sun, R. Camacho-Aguilera, L. C. Kimerling, and J. Michel, Opt. Lett. **35**, 679 (2010).
[20]X. Sun, J. Liu, L. C. Kimerling, and J. Michel, Opt. Lett. **34**, 1198 (2009).
[21]S.-L. Cheng, J. Lu, G. Shambat, H.-Y. Yu, K. Saraswat, J. Vuckovic, and Y. Nishi, Opt. Express **17**, 10019 (2009).
[22]R. Jakomin, G. Beaudoin, N. Gogneau, B. Lamare, L. Largeau, O. Mauguin, and I. Sagnes, "p and n-type Germanium layers grown using isobutyl germane in a III-V MOVPE reactor," Thin Solid Films (2010) (to be published).
[23]E. Woelk, D. V. Shenai-Khatkhate, R. L. DiCarlo, Jr., A. Amamchyan, M. B. Power, B. Lamare, G. Beaudoin, and I. Sagnes, J. Cryst. Growth **287**, 684 (2006).
[24]J. R. Haynes, Phys. Rev. **98**, 1866 (1955).
[25]W. van Roosbroeck and W. Schockley, Phys. Rev. **94**, 1558 (1954).
[26]Y. P. Varshni, Phys. Status Solidi **19**, 459 (1967).
[27]J. I. Pankove and P. Aigrain, Phys. Rev. **126**, 956 (1962).
[28]M. El Kurdi, S. David, X. Checoury, G. Fishman, P. Boucaud, O. Kermarrec, D. Bensahel, and B. Ghyselen, Opt. Commun. **281**, 846 (2008).
[29]T.-P. Ngo, M. El Kurdi, X. Checoury, P. Boucaud, J. F. Damlencourt, O. Kermarrec, and D. Bensahel, Appl. Phys. Lett. **93**, 241112 (2008).

Downloaded 28 Jul 2010 to 193.48.163.6. Redistribution subject to AIP license or copyright; see http://jap.aip.org/jap/copyright.jsp